Polysilane and related radical rearrangements: an *ab initio* study of (1,2)-silyl, germyl and stannyl translocations in radicals derived from trisilanes and related species †

Sonia M. Horvat and Carl H. Schiesser *

School of Chemistry, The University of Melbourne, Victoria, Australia 3010

Received (in Cambridge, UK) 3rd January 2001, Accepted 22nd March 2001
First published as an Advance Article on the web 26th April 2001

Ab initio molecular orbital calculations using a (valence) double-ζ pseudopotential basis set (DZP) with (MP2, QCISD) and without (SCF) the inclusion of electron correlation predict that the transition states (**5**, **7**) involved in homolytic (1,2)-translocation reactions of silyl (SiH_3), germyl (GeH_3) and stannyl (SnH_3) groups between silicon and other group (IV) centres proceed *via* homolytic substitution mechanisms involving frontside attack at the heteroatom undergoing translocation. At the highest level of theory (CCSD(T)/aug-cc-pVDZ//MP2/aug-cc-pVDZ), an energy barrier ($\Delta E^{\ddagger}$) of 135.9 kJ mol^{-1} is calculated for the translocation of SiH_3 between silicon centres; this value is 143.8 kJ mol^{-1} at the CCSD(T)/DZP//MP2/DZP level. Similar results are obtained at the CCSD(T)/DZP//MP2/DZP level of theory for reactions involving germanium and tin with values of $\Delta E^{\ddagger}$ of 146.5 and 129.1 kJ mol^{-1} respectively for the rearrangements of trigermapropyl and tristannapropyl radicals respectively. These data strongly suggest that homolytic (1,2)-translocation reactions are unlikely to be involved in the free-radical degradation of polysilanes, polygermanes and polystannanes. CCSD(T)/DZP//MP2/DZP calculated energy barriers associated with mixed systems range from 108.1 kJ mol^{-1} for the (1,2)-translocation of SnH_3 from tin to silicon, to 181.0 kJ mol^{-1} for the similar migration of SiH_3 from silicon to tin. The mechanistic implications of these observations are discussed.

Introduction

Polysilanes have interesting chemical and physical properties with benefit to a wide range of emerging technologies.[1] Often, these polymers are prepared by dehydrogenative coupling of silanes in the presence of metallocenes to give the poly(hydrosilane) structure **1**.[2] These poly(hydrosilane)s are readily functionalised by further reaction with suitable substrates such as terminal alkenes, aldehydes and ketones,[3] or can themselves be used as reagents for the free-radical reduction of organic halides.[4]

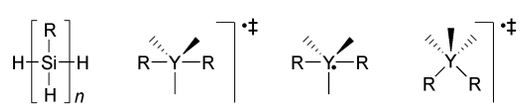

1 **2** **3** **4**

Of particular significance to chemical synthesis are the stability properties of **1**. Chatgilialoglu *et al.* reported recently that poly(hydrosilane)s are susceptible to autoxidation in a process predominantly involving a free-radical chain mechanism.[5] In addition, free-radical attack at tetravalent silicon appears to play an important role in the radical-based degradation of poly(phenylsilane).[6]

Homolytic substitution chemistry involving attack at saturated silicon, germanium and tin is not without precedent. For example, intramolecular (1,*n*) group transfer chemistry involving silyl, germyl and stannyl radicals can be useful in free-radical based synthesis.[7] Radical Brook-type rearrangements[8] and the 1,5- and 1,6-translocations reported by Kim and co-workers[9] are representative of this chemistry (Scheme 1); other examples can be found in recent reviews.[7,10]

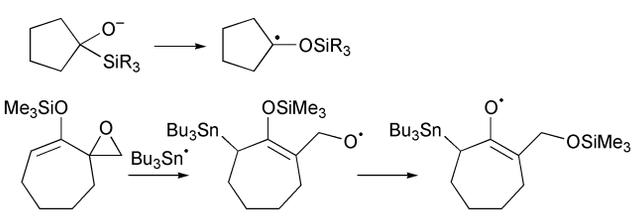

Scheme 1

Work in our laboratories has been directed toward the design, application and understanding of free-radical homolytic substitution chemistry with the aim of developing a novel synthetic methodology.[11] To that end, we published recently several *ab initio* studies with the aim of increasing our understanding of the factors which affect and control the mechanism of homolytic substitution at several main-group higher heteroatoms. It is generally agreed that homolytic substitution by a radical ($R^{\bullet}$) at a group (Y) proceeds either *via* a transition state (**2**) in which the attacking and leaving radicals adopt a collinear (or nearly so) arrangement resulting in Walden inversion, or with the involvement of a hypervalent intermediate (**3**) which may or may not undergo pseudorotation prior to dissociation.[7] Indeed, high-level *ab initio* calculations support this view for reactions involving free-radical attack at the pnicogens, chalcogens and halogens; reactions involving phosphorus[12] and tellurium[13] are predicted to involve intermediates, while those involving sulfur,[13] selenium[13] and the halogens[14] appear to proceed by direct displacement of the leaving radical.

In addition to the pathways for homolytic attack described above, a mechanism involving *frontside* attack *via* transition state **4** has also recently been investigated. Indeed, Dobbs and Doren explored the mechanism of the reaction of hydrogen atom with disilane and noted that *frontside* homolytic

† Electronic supplementary information (ESI) available: HF/6-311G**, HF/DZP, MP2/6-311G**, MP2,DZP, MP2/cc-pVDZ, MP2/aug-cc-pVDZ, B3LYP/6-311G** and B3LYP/DZP Gaussian Archive entries for the optimized structures in this study and higher-level calculated single-point energies. See http://www.rsc.org/suppdata/p2/b1/b100162k/

DOI: 10.1039/b100162k

substitution is more favorable than the analogous backside mechanism by 11.7 kJ mol^{-1} at the MP2/6-311G** level of theory.[15] This value correlates well with available experimental data.[16] Similar computational investigations into the mechanism of the radical Brook rearrangement concluded that 1,2-migrations involving group (IV) elements proceed *via* the *frontside* homolytic substitution mechanism,[17] while recent calculations revealed that both frontside and backside mechanisms have similar energy profiles for intermolecular reactions involving silicon, germanium and tin.[18]

As part of an ongoing interest in homolytic substitution chemistry involving main group higher heteroatoms, and in order to assess the stability of radicals generated from polysilanes and related systems toward free-radical rearrangement, we now report *ab initio* calculations on the intramolecular 1,2-homolytic transfer chemistry of silyl, germyl and stannyl groups between group (IV) centres and conclude that this chemistry is unlikely to play a role in the free-radical degradation of polysilanes.

Methods

Ab initio molecular orbital calculations were carried out using the Gaussian 94[19] or Gaussian 98[20] program. Geometry optimisations were performed using standard gradient techniques at the SCF, MP2 and B3LYP levels of theory using restricted (RHF, RMP2 and RB3LYP) and unrestricted (UHF, UMP2 and UB3LYP) methods for closed and open shell systems, respectively.[21] Further single-point QCISD and CCSD(T) calculations were performed on each of the MP2 optimised structures. When correlated methods were used, calculations were performed using the frozen core approximation. Except for MP2/aug-cc-pVDZ, whenever geometry optimisations were performed, vibrational frequencies were calculated to determine the nature of located stationary points. Calculations were performed on all reactants, products and transition states to obtain barriers and energies of reaction. Where appropriate, zero-point vibrational energy (ZPE) corrections have been applied. Values of $\langle s^2 \rangle$ never exceeded 0.86 before annihilation of quartet contamination and were mostly below 0.79 at correlated levels of theory.

Standard basis sets were used. In addition, the (valence) double-ζ pseudopotential basis set of Hay and Wadt[22] supplemented with a single set of *d*-type polarisation functions was used for the heteroatoms in this study (exponents $d(\zeta)_{Si} = 0.284$,[23] $d(\zeta)_{Ge} = 0.230$[23] and $d(\zeta)_{Sn} = 0.200$) while the double-ζ all-electron basis sets of Dunning and Hay[24] with an additional set of polarisation functions (exponents $d(\zeta)_C = 0.75$ and $p(\zeta)_H = 1.00$) were used for C and H. We refer to this basis set as DZP throughout this work.[13,14,18]

Calculations were performed on DEC AlphaStation 400 4/233, DEC Personal Workstation 433au or 600au, Compaq DS10 or NEC SX-4 computers.

Optimised geometries and energies for all structures in this study (Gaussian Archive entries) are available as Supplementary Material.

Results and discussion

(1,2)-Translocations between silicon, germanium, and tin centres. Degenerate rearrangements of the trisilapropyl, trigermapropyl and tristannapropyl radicals

Hypervalent species (**5**, Y = Z) of C_1 symmetry were located on the H_7Y_3 (Y = Si, Ge, Sn) potential energy surfaces at the UHF/DZP, MP2/DZP and B3LYP/DZP levels of theory. In addition, **5** (Y = Z = Si) was also optimised at the UHF/6-311G** and MP2/6-311G**, MP2/cc-pVDZ, MP2/aug-cc-pVDZ levels of theory. Analysis of the force constants associated with structures **5** (Y = Z) reveals that they correspond to the transition states for the degenerate rearrangement of the trisilapropyl, trigermapropyl, and tristannapropyl radicals (**6**, Y = Z) (Scheme 2). The important geometrical features of structures **5**

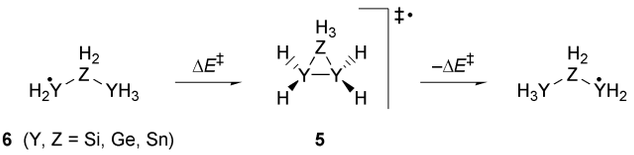

6 (Y, Z = Si, Ge, Sn) **5**

Scheme 2

are summarised in Fig. 1, while calculated energy barriers ($\Delta E^{\ddagger}$, Scheme 2) and corresponding imaginary frequencies are listed in Table 1. Full computational details are available as Supplementary Material.

Fig. 1 reveals that transition states **5** (Y = Z) resemble those located for analogous intermolecular homolytic substitution reactions involving the *frontside* mechanism[18] and the structures predicted to be involved in the (1,2)-migration of silicon, germanium and tin between carbon centres, between carbon and nitrogen, and between carbon and oxygen.[17] Depending on the element involved and the level of theory employed, transition states **5** (Y = Z) are predicted to involve attack angles that lie between 45 and 58°. These values are more severe than those found for the analogous intermolecular reactions,[18] the implications of this are discussed later. In addition, and as expected, the $(Y–Y)_{TS}$ distance increases in moving from silicon to germanium and tin. MP2/DZP calculations predict separations of 2.56 (Si), 2.75 (Ge), and 3.10 (Sn).

Inspection of Table 1 reveals that the transition state **5** (Y = Z = Si) associated with the (1,2)-transfer of silicon is calculated to lie some 187.5 kJ mol^{-1} above the reactant (**6**) using UHF/6-311G**. Inclusion of electron correlation in these calculations (MP2/6-311G**) serves to reduce this energy barrier to 155.0 kJ mol^{-1}, while inclusion of zero-point vibrational energy correction (ZPE) would appear to also lower the calculated energy barrier by approximately 5 kJ mol^{-1}. Further improvements in both basis set quality and correlation result in further reduction in $\Delta E^{\ddagger}$ which appears to converge to a value of about 135 kJ mol^{-1}. At the highest level of theory used (CCSD(T)/aug-cc-pVDZ//MP2/aug-cc-pVDZ), a barrier of 135.9 kJ mol^{-1} is predicted for the rearrangement of the trisilapropyl radical. It is interesting to compare this value with that calculated using the B3LYP density functional method; 131.7 kJ mol^{-1} is predicted at the B3LYP/6-311G** level, while B3LYP/DZP predicts a value of 133.3 kJ mol^{-1}.

Similar trends in energy are predicted for the (1,2)-transfer of germanium and tin, with CCSD(T)/DZP//MP2/DZP calculated barriers of 146.1 kJ mol^{-1} and 129.1 kJ mol^{-1} for the degenerate rearrangements of trigermapropyl (**6**, Y = Ge) and tristannapropyl (**6**, Y = Sn) radicals respectively.

As was observed in previous calculations,[17,18] at correlated levels of theory the (1,2)-migration of the germyl group in trigermapropyl radical is predicted to proceed with a higher energy barrier ($\Delta E^{\ddagger}$) than either reaction involving silicon or tin. This trend is most pronounced at the QCISD/DZP//MP2/DZP level, where values of $\Delta E^{\ddagger}$ range from 149.3 kJ mol^{-1} (Si), to 152.0 (Ge) and 134.3 kJ mol^{-1} (Sn).

Degenerate rearrangements of $H_3ZYH_2YH_2^{\bullet}$ (Y, Z = Si, Ge, Sn)

Extensive searching of the H_7Y_2Z (Y, Z = Si, Ge, Sn) potential energy surfaces at the SCF/DZP and MP2/DZP levels of theory located structures (**5**, Y ≠ Z) as transition states for the (1,2)-translocation of SiH_3, GeH_3, and SnH_3 in the 3-germa-1,2-disila-1-propyl, 3-stanna-1,2-disila-1-propyl, 1,2-digerma-3-sila-1-propyl, 1,2-digerma-3-stanna-1-propyl, 3-sila-1,2-distanna-1-propyl and 3-germa-1,2-distanna-1-propyl

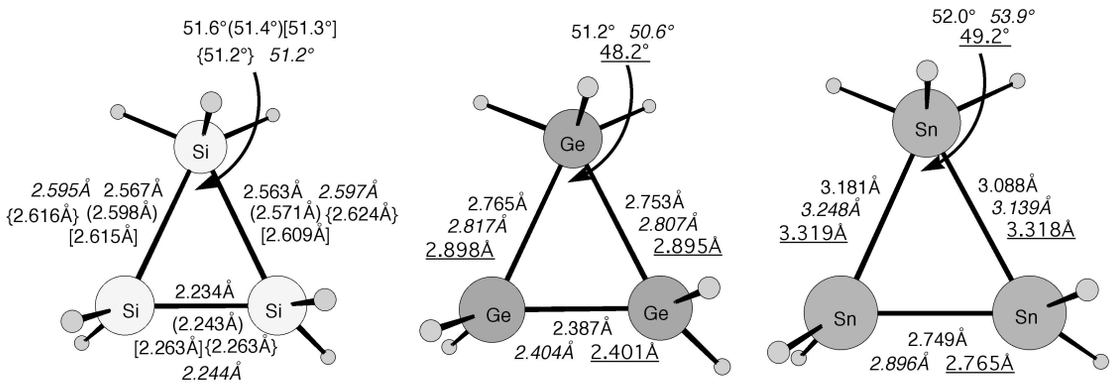

Fig. 1 Optimized structures of transition states **5** (Y = Z) for the degenerate rearrangements of the trisilapropyl, trigermapropyl and tristannapropyl radicals **6** (Y = Z). UHF/DZP, MP2/DZP (MP2/6-311G**) [MP2/cc-pVDZ] {MP2/aug-cc-pVDZ}, *B3LYP/DZP*.

Table 1 Calculated energy barriers[a] ($\Delta E^{\ddagger}$) for the degenerate (1,2)-translocation of SiH_3, GeH_3, and SnH_3, in trisilapropyl, trigermapropyl and tristannapropyl radicals (**6**) (Scheme 2) and imaginary frequencies (ν)[b] associated with transition states (**5**)

Y	Method	$\Delta E^{\ddagger}$	$\Delta E^{\ddagger}$ + ZPE	ν
Si	HF/6-311G**	187.5	182.0	603i
	HF/DZP	185.8	180.6	589i
	MP2/6-311G**	155.0	149.4	552i
	MP2/DZP	150.8	145.9	550i
	MP2/cc-pVDZ	146.3	141.7	544i
	MP2/aug-cc-pVDZ	141.9		
	QCISD/6-11G**//MP2/6-311G**	154.3	—	—
	QCISD/DZP//MP2/DZP	149.3	—	—
	QCISD/cc-pVDZ//MP2/cc-pVDZ	146.5	—	—
	QCISD/aug-ccpVDZ//MP2/aug-cc-pVDZ	142.5	—	—
	CCSD(T)/6-311G**//MP2/6-311G**	148.8	—	—
	CCSD(T)/DZP//MP2/DZP	143.8	—	—
	CCSD(T)/cc-pVDZ//MP2/cc-pVDZ	140.6	—	—
	CCSD(T)/aug-cc-pVDZ//MP2/aug-cc-pVDZ	135.9	—	—
	B3LYP/6-311G**	131.7	126.1	446i
	B3LYP/DZP	133.3	127.8	451i
Ge	HF/DZP	183.2	177.5	437i
	MP2/DZP	156.1	150.8	500i
	QCISD/DZP//MP2/DZP	152.0	—	—
	CCSD(T)/DZP//MP2/DZP	146.5	—	—
	B3LYP/DZP	136.6	130.4	373i
Sn	HF/DZP	159.9	154.2	302i
	MP2/DZP	140.3	135.1	384i
	QCISD/DZP//MP2/DZP	134.3	—	—
	CCSD(T)/DZP//MP2/DZP	129.1	—	—
	B3LYP/DZP	110.5	104.9	139i

[a] Energies in kJ mol^{-1}. [b] Frequencies in cm^{-1}.

radicals (**6**, Y ≠ Z) (Scheme 2). Structures (**5**, Y ≠ Z) proved, once again, to be of C_1 symmetry and are displayed in Fig. 2, while energy barriers ($\Delta E^{\ddagger}$) are listed in Table 2; full details are available as Supplementary Material.

Inspection of Table 2 and Fig. 2 reveals some interesting trends in energy and geometrical features which may help in our understanding of the high barriers associated with the intramolecular (1,2)-migration of the group (IV) elements in this study.

The MP2/DZP (Y–Z) distances in the transition states (**5**, Y ≠ Z) are calculated to lie between 2.65 (Si–Ge) and 3.02 Å (Ge–Sn). It is interesting to compare these distances with those calculated at the same level of theory for the transition states involved in the analogous intermolecular homolytic substitution reaction by the frontside attack mechanism at the same level of theory.[18] For example, distances of 2.56 (Si–Ge), 2.75 (Si–Sn) and 2.86 Å (Ge–Sn) are obtained in the analogous transition states (**4**),[13] indicating that the strain engendered in transition states **5** leads, not unexpectedly, to some lengthening of the transition state separations when compared to structures **4**.

As was observed for the other degenerate reactions in this study, the relatively large Y–Z separations in transition states (**5**, Y ≠ Z) lead to substantial deviations in attack angle from those predicted for the analogous intermolecular transition states. As Fig. 2 displays, the Y–Z–Y angle becomes increasingly more severe as the X–Y distance increases. MP2/DZP calculations predict angles which range from 47 (X = Si, Y = Sn) to 56° (X = Sn, Y = Si). The similar angle for the analogous intermolecular reaction is calculated to lie at around 80°.

Table 2 clearly reveals that the (1,2)-translocations of silyl, germyl and stannyl groups between silicon, germanium and tin centres are predicted to have significant energy barriers, similar to those predicted for the analogous degenerate rearrangement of the trisilapropyl, trigermapropyl and tristannapropyl radicals (Scheme 2) and some 70 kJ mol^{-1} higher than those calculated for the analogous intermolecular reactions.[13] Not unexpectedly, values of $\Delta E^{\ddagger}$ are dependent on the nature of the attacking radical and the heteroatom undergoing homolytic substitution. For example, at the highest level of theory used, namely CCSD(T)/DZP//MP2/DZP, a value of 160.1 kJ mol^{-1} is obtained for the translocation of SnH_3 between silicon centres,

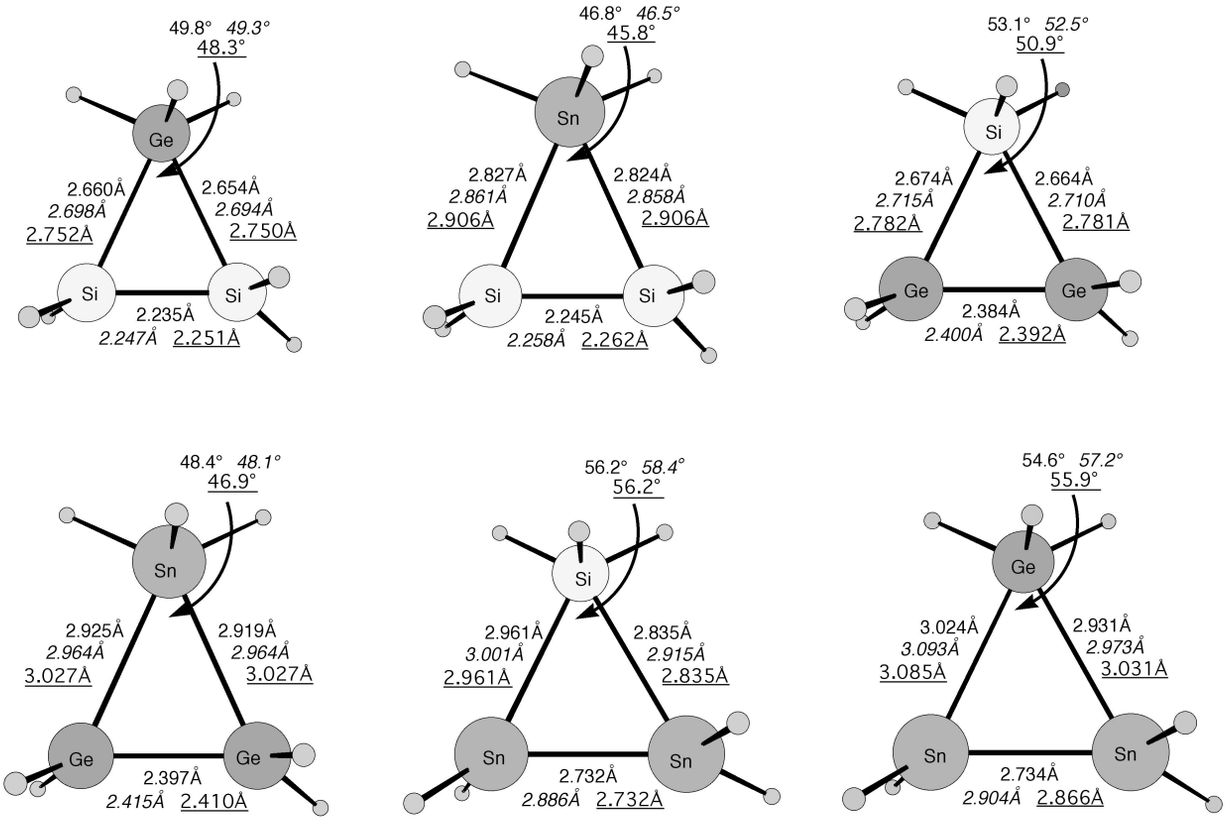

Fig. 2 MP2/DZP Optimized structures of transition states **5** (Y ≠ Z) for the degenerate rearrangements of radicals **6** (Y ≠ Z). *B3LYP/DZP Data in italics.* UHF/DZP Data underlined.

Table 2 Calculated energy barriers ($\Delta E^{\ddagger}$)[a] for the degenerate (1,2)-translocation of SiH_3, GeH_3, and SnH_3, in **6** (Y ≠ Z) (Scheme 2) and imaginary frequencies (ν)[b] associated with transition states (**5**, Y ≠ Z)

Y	Z	Method	$\Delta E^{\ddagger}$	$\Delta E^{\ddagger}$ + ZPE	ν
Si	Ge	HF/DZP	178.3	173.6	533i
		MP2/DZP	146.9	142.7	526i
		QCISD/DZP//MP2/DZP	144.3	—	—
		CCSD(T)/DZP//MP2/DZP	138.9	—	—
		B3LYP/DZP	129.0	124.5	417i
Si	Sn	HF/DZP	140.6	142.1	425i
		MP2/DZP	119.9	116.0	433i
		QCISD/DZP//MP2/DZP	116.8	—	—
		CCSD(T)/DZP//MP2/DZP	112.1	—	—
		B3LYP/DZP	104.9	106.2	333i
Ge	Si	HF/DZP	193.1	201.2	526i
		MP2/DZP	161.7	155.8	542i
		QCISD/DZP//MP2/DZP	159.0	—	—
		CCSD(T)/DZP//MP2/DZP	153.5	—	—
		B3LYP/DZP	142.3	135.5	419i
Ge	Sn	HF/DZP	153.2	147.5	348i
		MP2/DZP	129.4	124.4	380i
		QCISD/DZP//MP2/DZP	125.3	—	—
		CCSD(T)/DZP//MP2/DZP	120.6	—	—
		B3LYP/DZP	111.8	106.2	283i
Sn	Si	HF/DZP	195.1	188.6	446i
		MP2/DZP	171.9	166.0	557i
		QCISD/DZP//MP2/DZP	166.3	—	—
		CCSD(T)/DZP//MP2/DZP	160.1	—	—
		B3LYP/DZP	132.7	127.2	215i
Sn	Ge	HF/DZP	185.0	179.3	477i
		MP2/DZP	164.9	159.4	518i
		QCISD/DZP//MP2/DZP	158.3	—	—
		CCSD(T)/DZP//MP2/DZP	152.3	—	—
		B3LYP/DZP	126.4	121.2	165i

[a] Energies in kJ mol^{-1}. [b] Frequencies in cm^{-1}.

while 120.6 kJ mol^{-1} is calculated for the translocation of SiH_3 between tin centres. These values are reduced to 132.7 and 111.8 kJ mol^{-1} at the B3LYP/DZP level of theory. The trends observed in Table 2 are consistent with those calculated previously for intermolecular homolytic substitution.[13] They also reflect the known ability of silicon, germanium and tin centred radicals to become involved in substitution chemistry (*viz.* Si > Ge > Sn) and the ability of the various group (IV) elements to undergo radical substitution (*viz.* Sn = Ge > Si).[7]

Non-degenerate rearrangements of $H_3ZYH_2YH_2^{\bullet}$ (Y, Z = Si, Ge, Sn)

Transition states **7** for the non-degenerate (1,2)-translocations of the remaining radicals (**8**) in this study were located at the same levels of theory described previously. Important structural features are listed in Fig. 3, while the calculated energy barriers for the forward ($\Delta E_1^{\ddagger}$) and reverse ($\Delta E_2^{\ddagger}$) reactions (Scheme 3) are listed in Table 3 together with the (imaginary) transition state frequency calculated for transition states **7**.

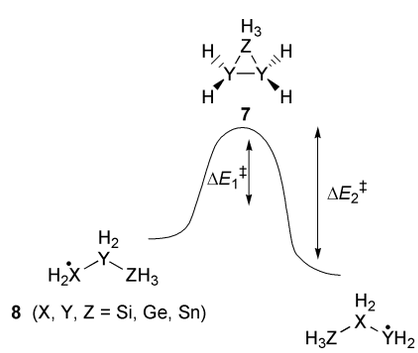

Scheme 3

Inspection of Fig. 3 reveals features which aid in our understanding of the reactions in question. Firstly, it is clear that reactions involving attack of a silicon-centred radical at

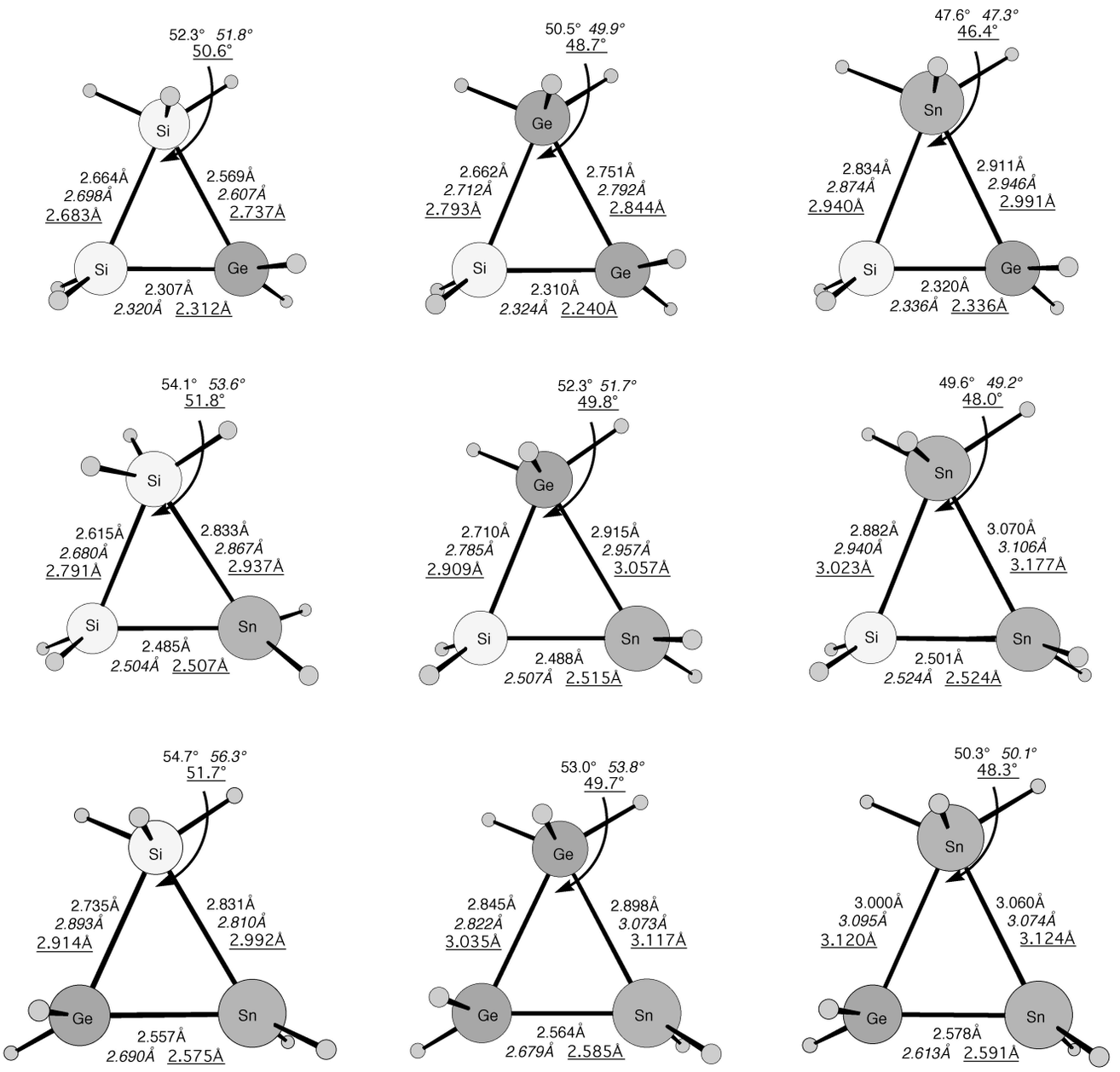

Fig. 3 MP2/DZP Optimized structures of transition states **7** for the non-degenerate rearrangements of radicals **8**. *B3LYP/DZP Data in italics.* UHF/DZP Data underlined.

germanium and tin are "earlier" than those involving attack of germanium or tin at the same heteroatom. For example, the Si–Si separation in **7** (X = Z = Si, Y = Ge) is calculated to be 2.664 Å at the MP2/DZP level of theory, longer than the Si–Ge distance in the same transition state (2.569 Å), and is consistent with the relative reactivity of the attacking and leaving radicals in question. By comparison, the Si–Si distance in **5** (X = Y = Si) is about 2.56 Å. When the leaving radical is tin-centred as in **7** (X = Z = Si, Y = Ge), the transition state becomes even "earlier", with an MP2/DZP calculated Si–Si separation of 2.615 Å. This trend is reflected in all of the transition structures **7** and in the energy barriers ($\Delta E_1^{\ddagger}$, $\Delta E_2^{\ddagger}$) for the forward and reverse reactions. For example, at the CCSD(T)/DZP//MP2/DZP level, $\Delta E_1^{\ddagger}$ for the reaction involving **6** (X = Y = Si) is calculated to be 143.8 kJ mol^{-1}. When the leaving radical is germanium-centred as in **8** (X = Y = Si, Z = Ge) or tin-centred as in **8** (X = Y = Si, Z = Sn), this value is reduced to 138.2 and 134.4 kJ mol^{-1} respectively. In the reverse reactions where the attacking radical is varied from silicon to germanium and tin, the barriers ($\Delta E_2^{\ddagger}$) are calculated to be 143.8, 160.2 and 181.0 kJ mol^{-1} respectively. These observations are in accord with previously established trends for homolytic substitution involving group (IV) elements.[7,13] Similar observations can be made among other species in the series from the data presented in Table 3.

Conclusions

Ab initio calculations suggest homolytic (1,2)-translocations of silyl, germyl and stannyl groups between group (IV) elements are unlikely processes under standard conditions. CCSD(T)/DZP//MP2/DZP calculated energy barriers range from 108 kJ mol^{-1} for the translocation of SnH_3 from tin to silicon, to 181 kJ mol^{-1} for the migration of SiH_3 from silicon to tin. At all levels of theory, the transition states (**5**, **7**) are predicted to adopt geometries consistent with a *frontside* mechanism for migration. The high energy barriers (in excess of 120 kJ mol^{-1}) calculated for silyl migration suggest that reactions of this type are unlikely to be associated with free-radical degradation of polysilanes.

It is also instructive to comment on the B3LYP data generated in this study. Previous work has questioned the ability of density functional methods to adequately reproduce the energy

Table 3 Calculated energy barriers[a] ($\Delta E^{\ddagger}$) for the non-degenerate (1,2)-translocation of SiH_3, GeH_3, and SnH_3, in **8** (Scheme 3) and imaginary frequencies (ν)[b] associated with transition states **7**

X	Y	Z	Method	$\Delta E_1^{\ddagger}$	$\Delta E_1^{\ddagger}$ + ZPE	$\Delta E_2^{\ddagger}$	$\Delta E_2^{\ddagger}$ + ZPE	ν
Si	Ge	Si	HF/DZP	181.0	176.0	199.9	193.8	557i
			MP2/DZP	145.6	140.7	167.5	161.7	510i
			QCISD/DZP//MP2/DZP	143.9	—	165.6	—	—
			CCSD(T)/DZP//MP2/DZP	138.2	—	160.2	—	—
			B3LYP/DZP	128.2	122.5	148.4	141.8	405i
Si	Ge	Ge	HF/DZP	173.4	168.8	190.0	184.3	489i
			MP2/DZP	142.1	137.9	161.6	156.3	491i
			QCISD/DZP//MP2/DZP	139.4	—	158.3	—	—
			CCSD(T)/DZP//MP2/DZP	133.7	—	152.9	—	—
			B3LYP/DZP	124.6	119.6	142.5	136.5	379i
Si	Ge	Sn	HF/DZP	144.4	140.0	156.8	151.5	392i
			MP2/DZP	117.3	113.3	132.8	127.9	386i
			QCISD/DZP//MP2/DZP	114.0	—	129.2	—	—
			CCSD(T)/DZP//MP2/DZP	109.2	—	124.6	—	—
			B3LYP/DZP	90.6	96.6	104.5	109.7	295i
Si	Sn	Si	HF/DZP	177.4	172.3	216.6	209.0	532i
			MP2/DZP	142.1	137.5	190.5	183.4	485i
			QCISD/DZP//MP2/DZP	140.5	—	186.4	—	—
			CCSD(T)/DZP//MP2/DZP	134.3	—	181.0	—	—
			B3LYP/DZP	124.9	118.1	167.2	158.9	392i
Si	Sn	Ge	HF/DZP	170.6	165.9	203.1	196.0	448i
			MP2/DZP	139.8	135.8	181.6	175.2	478i
			QCISD/DZP//MP2/DZP	136.8	—	175.9	—	—
			CCSD(T)/DZP//MP2/DZP	130.7	—	170.7	—	—
			B3LYP/DZP	121.5	116.3	158.1	150.8	367i
Si	Sn	Sn	HF/DZP	145.3	140.9	168.7	162.3	368i
			MP2/DZP	116.8	112.7	150.8	144.7	371i
			QCISD/DZP//MP2/DZP	113.4	—	144.9	—	—
			CCSD(T)/DZP//MP2/DZP	108.1	—	166.6	—	—
			B3LYP/DZP	100.2	95.0	129.0	122.0	277i
Ge	Sn	Si	HF/DZP	185.2	179.6	205.6	198.5	485i
			MP2/DZP	155.2	149.9	181.7	174.9	569i
			QCISD/DZP//MP2/DZP	151.6	—	175.9	—	—
			CCSD(T)/DZP//MP2/DZP	145.5		170.4	—	—
			B3LYP/DZP	122.5	118.4	145.5	140.0	242i
Ge	Sn	Ge	HF/DZP	176.4	171.0	192.4	185.6	383i
			MP2/DZP	150.6	145.7	173.0	166.7	520i
			QCISD/DZP//MP2/DZP	145.5	—	165.7	—	—
			CCSD(T)/DZP//MP2/DZP	139.6	—	160.3	—	—
			B3LYP/DZP	118.1	110.3	136.9	128.0	292i
Ge	Sn	Sn	HF/DZP	151.4	146.5	162.5	156.6	325i
			MP2/DZP	126.4	121.6	145.0	139.2	391i
			QCISD/DZP//MP2/DZP	121.8	—	138.2	—	—
			CCSD(T)/DZP//MP2/DZP	116.5	—	133.5	—	—
			B3LYP/DZP	108.1	102.4	123.0	116.3	276i

[a] Energies in kJ mol^{-1}. [b] Frequencies in cm^{-1}.

surfaces associated with several classes of free-radical reaction.[25,26] Indeed, B3LYP provided energy data significantly different from those provided by high-level correlation methods for free-radical decarbonylation chemistry,[25] while a comprehensive study performed in our laboratories revealed little correlation between density functional method employed and the ability to accurately predict the nature of the stationary point (*i.e.* transition state *vs.* hypervalent intermediate) in homolytic substitution reactions involving chalcogen.[26] In this study, B3LYP/6-311G** appears to, once again, provide energy barriers consistently lower than those provided by correlated levels of theory. At the CCSD(T)/aug-cc-pVDZ//MP2/aug-cc-pVDZ level, this difference is only about 4 kJ mol^{-1}, while the difference between B3LYP/DZP and CCSD(T)/DZP//MP2/DZP is about 10 kJ mol^{-1}. Importantly, B3LYP/DZP appears to provide geometries for structures in this study consistent with those obtained at other levels and is able to reproduce the nature of the stationary point, although the imaginary frequencies obtained with B3LYP are smaller than those available from other methods.

Acknowledgements

We thank the Australian Research Council for financial support. We also gratefully acknowledge the support of the Melbourne Advanced Research Computing Centre.

References

1 *Silicon-Based Polymer Science: A Comprehensive Resource*, Eds. J. M. Ziegler and F. W. G. Fearon, Advances in Chemistry Series 224, American Chemical Society, Washington, DC, 1990.
2 J. F. Harrod, in *Progress in Catalysis*, Eds. K. J. Smith and E. C. Sanford, Elsevier, Amsterdam, 1992.

3 Y.-L. Hsiao and R. Waymouth, *J. Am. Chem. Soc.*, 1994, **116**, 9779.
4 C. Chatgilialoglu, C. Ferreri, D. Vechi, M. Lucarini and G. F. Pedulli, *J. Organomet. Chem.*, 1997, **545/546**, 455. See also: O. Yamazaki, H. Togo, S. Matsubayashi and M. Yokoyama, *Tetrahedron Lett.*, 1998, **39**, 1921; O. Yamazaki, H. Togo and M. Yokoyama, *J. Chem. Soc., Perkin Trans. 1*, 1999, 2891.
5 C. Chatgilialoglu, A. Guerrini, M. Lucarini, G. F. Pedulli, P. Carrozza, G. Da Roit, V. Borzatta and V. Lucchini, *Organometallics*, 1998, **17**, 2169.
6 C. Chatgilialoglu and A. Barbieri, manuscript in preparation.
7 C. H. Schiesser and L. M. Wild, *Tetrahedron*, 1996, **52**, 13256.
8 J. C. Dalton and R. A. Bourque, *J. Am. Chem. Soc.*, 1981, **103**, 699; Y.-M. Tsai and C.-D. Cherng, *Tetrahedron Lett.*, 1991, **32**, 3515.
9 S. Kim and J. S. Koh, *J. Chem. Soc., Chem. Commun.*, 1992, 1377; S. Kim, S. Lee and J. S. Koh, *J. Am. Chem. Soc.*, 1991, **113**, 5106; S. Kim and K. M. Lim, *J. Chem. Soc., Chem. Commun.*, 1993, 1152; S. Kim and K. M. Lim, *Tetrahedron Lett.*, 1993, **34**, 4851; S. Kim, J. Y. Do and K. M. Lim, *J. Chem. Soc., Perkin Trans. 1*, 1994, 2517; S. Kim, J. Y. Do and K. M. Lim, *Chem. Lett.*, 1996, 669; S. Kim, M. S. Jung, C. H. Cho and C. H. Schiesser, *Tetrahedron Lett.*, 2001, **43**, 943.
10 J. C. Walton, *Acc. Chem. Res.*, 1998, **31**, 99. See also: B. P. Roberts, *J. Chem. Soc., Perkin Trans. 2*, 1996, 2719.
11 C. H. Schiesser and K. Sutej, *Tetrahedron Lett.*, 1992, **33**, 5137; J. E. Lyons, C. H. Schiesser and K. Sutej, *J. Org. Chem.*, 1993, **58**, 5632; L. J. Benjamin, C. H. Schiesser and K. Sutej, *Tetrahedron*, 1993, **49**, 2557; M. C. Fong and C. H. Schiesser, *Tetrahedron Lett.*, 1995, **36**, 7329; M. A. Lucas and C. H. Schiesser, *J. Org. Chem.*, 1996, **61**, 5754; M. C. Fong and C. H. Schiesser, *J. Org. Chem.*, 1997, **62**, 3103; M. J. Laws and C. H. Schiesser, *Tetrahedron Lett.*, 1997, **38**, 8429; M. A. Lucas and C. H. Schiesser, *J. Org. Chem.*, 1998, **63**, 3032; L. Engman, M. J. Laws, J. Malmström, C. H. Schiesser and L. M. Zugaro, *J. Org. Chem.*, 1999, **64**, 6764; M. A. Lucas, O. T. K. Nguyen, C. H. Schiesser and S.-L. Zheng, *Tetrahedron*, 2000, **56**, 3995.
12 C. H. Schiesser and L. M. Wild, *Aust. J. Chem.*, 1995, **48**, 175. See also: J. M. Howell and J. F. Olsen, *J. Am. Chem. Soc.*, 1976, **98**, 7119; C. J. Cramer, *J. Am. Chem. Soc.*, 1990, **112**, 7965; C. J. Cramer, *J. Am. Chem. Soc.*, 1991, **113**, 2439.
13 K. F. Ferris, J. A. Franz, C. Sosa and R. J. Bartlett, *J. Org. Chem.*, 1992, **57**, 777; J. E. Lyons and C. H. Schiesser, *J. Chem. Soc., Perkin Trans. 2*, 1992, 1655; J. E. Lyons and C. H. Schiesser, *J. Organomet. Chem.*, 1992, **437**, 165; B. A. Smart and C. H. Schiesser, *J. Chem. Soc., Perkin Trans. 2*, 1994, 2269; C. H. Schiesser and B. A. Smart, *Tetrahedron*, 1995, **51**, 6051; C. H. Schiesser, B. A. Smart and T.-A. Tran, *Tetrahedron*, 1995, **51**, 10651; C. H. Schiesser and B. A. Smart, *J. Comput. Chem.*, 1995, **16**, 1055; C. H. Schiesser and M. A. Skidmore, *Chem. Commun.*, 1996, 1419; C. H. Schiesser and M. A. Skidmore, *J. Organomet. Chem.*, 1998, **552**, 145; C. H. Schiesser and L. M. Wild, *J. Org. Chem.*, 1999, **64**, 1131.
14 C. H. Schiesser, B. A. Smart and T.-A. Tran, *Tetrahedron*, 1995, **51**, 3327; C. H. Schiesser and L. M. Wild, *J. Org. Chem.*, 1998, **63**, 670.
15 K. D. Dobbs and D. J. Doren, *J. Am. Chem. Soc.*, 1993, **115**, 3731.
16 L. Fabry, P. Potzinger, B. Reimann, A. Ritter and H. P. Steenberger, *Organometallics*, 1986, **5**, 1231.
17 C. H. Schiesser and M. L. Styles, *J. Chem. Soc., Perkin Trans. 2*, 1997, 2335.
18 S. M. Horvat, C. H. Schiesser and L. M. Wild, *Organometallics*, 2000, **19**, 1239. See also: C. H. Schiesser, M. L. Styles and L. M. Wild, *J. Chem. Soc., Perkin Trans. 2*, 1996, 2257.
19 Gaussian 94, Revision B.3, M. J. Frisch, G. G. Trucks, B. Schlegel, P. M. W. Gill, B. G. Johnson, M. A. Robb, J. R. Cheeseman, T. Keith, G. A. Petersson, J. A. Montgomery, K. Raghavachari, M. A. Al-Laham, V. G. Zakrzewski, J. V. Ortiz, J. B. Foresman, C. Y. Peng, P. Y. Ayala, W. Chen, M. W. Wong, J. L. Andres, E. S. Replogle, R. Gomperts, R. L. Martin, D. J. Fox, J. S. Binkley, D. J. Defrees, J. Baker, J. J. P. Stewart, M. Head-Gordon, C. Gonzalez and J. A. Pople, Gaussian Inc., Pittsburgh, PA, 1995.
20 Gaussian 98, Revision A.7, M. J. Frisch, G. W. Trucks, H. B. Schlegel, G. E. Scuseria, M. A. Robb, J. R. Cheeseman, V. G. Zakrzewski, J. A. Montgomery, Jr., R. E. Stratmann, J. C. Burant, S. Dapprich, J. M. Millam, A. D. Daniels, K. N. Kudin, M. C. Strain, O. Farkas, J. Tomasi, V. Barone, M. Cossi, R. Cammi, B. Mennucci, C. Pomelli, C. Adamo, S. Clifford, J. Ochterski, G. A. Petersson, P. Y. Ayala, Q. Cui, K. Morokuma, D. K. Malick, A. D. Rabuck, K. Raghavachari, J. B. Foresman, J. Cioslowski, J. V. Ortiz, A. G. Baboul, B. B. Stefanov, G. Liu, A. Liashenko, P. Piskorz, I. Komaromi, R. Gomperts, R. L. Martin, D. J. Fox, T. Keith, M. A. Al-Laham, C. Y. Peng, A. Nanayakkara, C. Gonzalez, M. Challacombe, P. M. W. Gill, B. Johnson, W. Chen, M. W. Wong, J. L. Andres, M. Head-Gordon, E. S. Replogle and J. A. Pople, Gaussian, Inc., Pittsburgh, PA, 1998.
21 W. J. Hehre, L. Radom, P. v. R. Schleyer and P. A. Pople, *Ab Initio Molecular Orbital Theory*, Wiley, New York, 1986.
22 W. R. Wadt and P. J. Hay, *J. Chem. Phys.*, 1985, **82**, 284; P. J. Hay and W. R. Wadt, *J. Chem. Phys.*, 1985, **82**, 270; P. J. Hay and W. R. Wadt, *J. Chem. Phys.*, 1985, **82**, 299.
23 A. Höllwarth, M. Böhme, S. Dapprich, A. W. Ehlers, A. Gobbi, V. Jonas, K. F. Köhler, R. Stegmann, A. Veldkamp and G. Frenking, *Chem. Phys. Lett.*, 1993, **208**, 237.
24 T. H. Dunning and P. J. Hay, *Modern Theoretical Chemistry*, 1976, Plenum, New York, ch. 1, pp. 1–28.
25 T. Morihovitis, C. H. Schiesser and M. A. Skidmore, *J. Chem. Soc., Perkin Trans. 2*, 1999, 2041.
26 C. H. Schiesser and M. A. Skidmore, unpublished results.